J|A|C|S
COMMUNICATIONS

Published on Web 12/10/2002

A Dihydroxo-Bridged Fe(II)−Fe(III) Complex: A New Member of the Diiron Diamond Core Family

Rune Kirk Egdal,[†] Alan Hazell,[‡] Frank Bartnik Larsen,[†] Christine J. McKenzie,*[,†] and Robert C. Scarrow*[,§]

Department of Chemistry, University of Southern Denmark, Odense Campus, 5230 Odense M, Denmark, Department of Chemistry, Aarhus University, 8000 Århus, Denmark, and Department of Chemistry, Haverford College, 370 Lancaster Avenue, Haverford, Pennsylvania 19041-1392

Received June 7, 2002; E-mail: chk@chem.sdu.dk

Dinuclear iron complexes with a $M_2(\mu\text{-}O)_2$ "diamond core" have received considerable attention due to their importance as structural, spectroscopic, and functional models for the active site of the hydroxylation protein in methane monoxygenase (MMOH).[1] The most extensive series of diamond cores are those with neutral N_4 capping ligands, Scheme 1, A (6-Me$_3$-TPA),[1c,2] B (6-Me$_3$-TPA, BQPA, BPEEN),[1d,e,2] C (6-Me$_3$-TPA),[1d,e] and D (5-Et$_3$-TPA).[1f,2] We report here a mixed-valence $Fe^{II}-Fe^{III}$ diamond core which is missing from the series. Notably, a mixed-valence $Fe^{II}-Fe^{III}$ oxidation state ($MMOH_{mv}$) has been recently structurally characterized for MMOH, and a core μ-OH-μ-OH_2 structure was assigned.[3]

Scheme 1

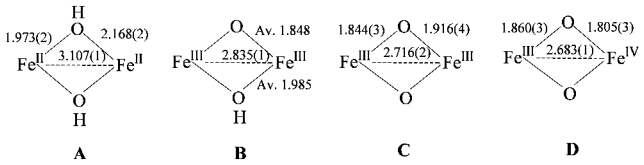

Green rhombohedral crystals of $[L_2Fe_2(OH)_2](ClO_4)_3 \cdot 3H_2O$, L = *N*,*N*′-dimethyl-*N*,*N*′-bis(2-pyridylmethyl)ethane-1,2-diamine (**1**), are deposited over several days from solutions containing anhydrous $FeCl_2$ and $L \cdot 2HClO_4$ in 1:1 proportions in acetonitrile:water. The reaction was carried out under nitrogen; however, this may not have been sufficiently strict since dioxygen is a likely source of the oxidant required for the reaction. Isolation of **1** is dependent on pH and the use of anhydrous $FeCl_2$ as iron source. If one equivalent of sodium hydroxide is added, red crystals of the single μ-oxo-bridged diiron(III) chloride complex $[L_2Fe_2(\mu\text{-}O)Cl_2](ClO_4)_2$ are isolated.[4] Complex **1** is formally related to the oxo-hydroxo bridged diiron(III) complex $[L_2Fe_2(O)(OH)](ClO_4)_3$ (**2**)[5] and two crystallographically characterized compounds containing other N_4 capping ligands[1d,e] by the reductive addition of one H$^\bullet$ to the core. The near-IR spectrum of **1** in acetonitrile shows a broad ($\Delta\nu_{1/2} \approx 4300$ cm^{-1}) band centered at 1180 nm ($\epsilon = 70$ M^{-1} cm^{-1}) which we assign to an IVCT absorption. Upon opening the solution to air, this band disappears over the course of 20 min, indicating, perhaps not surprisingly, that **1** is not stable in aerobic solution.

A comparison of the XANES of **1** with that of the diferric complex, $[L(HO)Fe(O)Fe(OH_2)L](ClO_4)_3$ (**3**)[6] shows that the energy of the K edge for **1** is between that of **3** and that of iron(II) coordination compounds (Figure 1a). The 1s → 3d pre-edge peak near 7113 eV is broader than usually observed for iron complexes but can be curve-fit[7] by two Gaussian peaks at energies typical for iron(II) and iron(III) complexes, respectively (Figure 1a). This

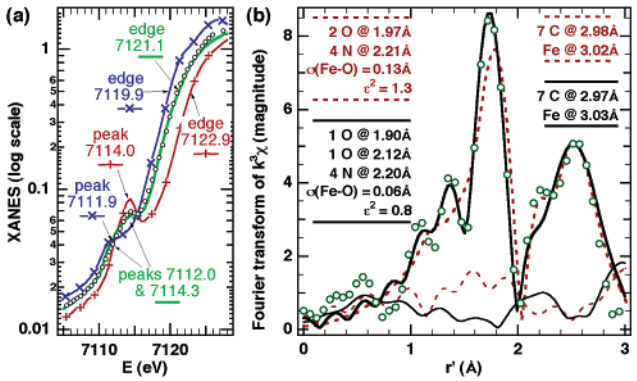

Figure 1. (A) XANES of **1** (−, green), $Fe^{II}(N\text{-}MeIm)_6[BF_4]_2$ [2] (− × −, blue) and **3** (− + −, red). Also shown is the average of the spectra of $Fe^{II}(N\text{-}MeIm)_6[BF_4]_2$ and **3** (○○○). Edge positions (XANES = 0.50) and 1s → 3d pre-edge peak positions obtained from simulations are indicated. (B) FT EXAFS of **1** (○○○) and fits discussed in text. Magnitude of the FT simulations (upper lines) and residuals (lower lines) are shown. Details and more graphs of EXAFS fits may be found in the Supporting Information.

suggests a valence-localized model with 50% Fe^{II} and 50% Fe^{III} sites; in fact, as shown by Figure 1a, the XANES of **1** is almost exactly an average of the XANES for diferric **3** and an iron(II)−imidazole complex. This behavior contrasts to that expected for a delocalized $Fe^{2.5+}$ dimer, where the 1s → 3d peak is expected at an intermediate energy but with roughly the same width as observed for Fe^{II} and Fe^{III} compounds, and where the XANES would differ from an average of an Fe^{II} and Fe^{III} spectrum. A recent example of this contrasting behavior is found in the XANES for a carboxylate-bridged $Fe^{2.5+}$ dimer, $[Fe_2(\mu\text{-}O_2CAr^{Tol})_4(4\text{-}^tBuC_5H_4N)_2]$.[8]

EXAFS analysis[9] also supports valence localization in **1** (Figure 1b). The EXAFS can be fit with a shell of two Fe−O bonds of 1.97 Å and another shell of four Fe−N bonds. However, the refined $\sigma = 0.13$ Å (Debye−Waller factor) for the Fe−O shell is too large for purely vibrational disorder, suggesting some Fe−O bonds are longer and some shorter than the average of 1.97 Å. A better fit (Figure 1b) and reasonable vibrational σ (0.06 Å) is obtained by refining one Fe−O bond (per iron) to 1.90(3) Å and the other to 2.12(8) Å.[9] These bond lengths are assigned to the Fe−O bonds of Fe^{3+} and Fe^{2+}, respectively.

The X-ray crystal structure of the cation in **1**[10] is shown in Figure 2a. The iron atoms are 2.952(1) Å apart and are bisected by a C_2 symmetry axis. The structure is of high enough quality that the hydrogen atoms of the bridging hydroxides were found in the difference Fourier synthesis; these form a H-bond to a lattice water molecule as shown. Anisotropic refinement of the electron density of the hydroxide oxygen atom gave an elongated thermal ellipsoid. An alternate and equally good fit to the electron density ($R_w = 0.044$) was obtained using two-half-occupancy isotropic atoms (O1a

[†] University of Southern Denmark.
[‡] Aarhus University.
[§] Haverford College.

10.1021/ja027219t CCC: $25.00

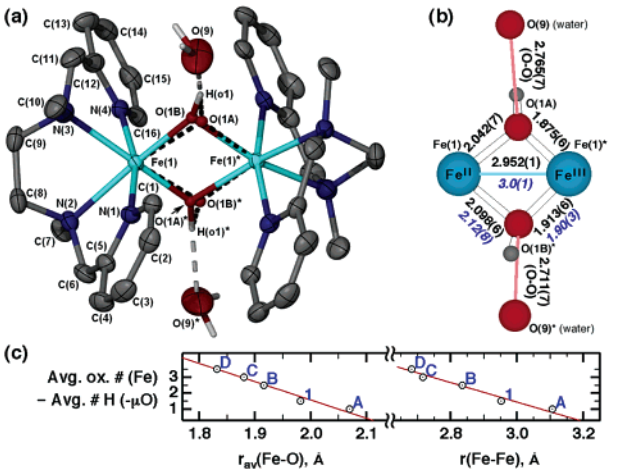

Figure 2. (a) X-ray crystallographic structure of the cation of **1**, drawn with 50% probability thermal ellipsoids, except for the disordered μ-OH oxygen atoms drawn with radius = 0.15 Å. H atoms other than H(o1), the only H atom located using the difference Fourier synthesis, are omitted for clarity. (b) Chem 3D representation of one of the half-occupancy core structures. EXAFS-derived distances are in blue italics. Other crystallographic distances (Å) and angles: Fe···Fe, 2.952(1), Fe(1)−N(1) 2.162(4), Fe(1)−N(2) 2.216(3), Fe(1)−N(3) 2.234(3), Fe(1)−N(4) 2.165(4), Fe(1)−O(1A)−Fe(1)* 97.7(3)°, Fe(1)−O(1B)*−Fe(1)* 94.7(3)°, O(1A)−Fe(1)−O(1B)* 79.1(2)°, O(1A)−Fe(1)*−O(1B)* 88.2(2)°. (c) Trends in average Fe−O and Fe−Fe distances of Fe_2O_2 cores of **1** and complexes represented in Scheme 1.

and O1b) placed about 0.2 Å apart. Because of its consistency with the XANES and EXAFS analyses, the latter structural model is preferred and shown in Figure 2. The four crystallographic Fe−O distances include two at an average of 1.894(6) Å and two averaging to 2.070(7), consistent with the EXAFS-derived distances and those expected for Fe^{III}−μ-OH and Fe^{II}−μ-OH, respectively.

A comparison of interatomic core distances for **1** obtained by X-ray crystallography and EXAFS is shown in Figure 2b. The thermal elipsoids of the N atoms, as well as the EXAFS disorder factor (σ) for the Fe−N shell (0.08 Å), are small, indicating that any shortening of the Fe−N bonds from the Fe^{II} to Fe^{III} side of the complex is minor. Thus, bond length changes from the Fe^{III} to Fe^{II} side of the complex are localized in the Fe−O bonds. Precedent for this is found in a search of the Cambridge Structural Database[11] for high-spin non-heme complexes with O_2N_4 coordination. The average Fe−N distance changes only slightly, from 2.20 Å in Fe^{II} complexes to 2.16 Å in Fe^{III} complexes, while the average Fe−O distance decreases by 0.2 Å from 2.10 Å (Fe^{II}) to 1.91 Å (Fe^{III}).

Complex **1** extends the series of $Fe_2(OH_x)_2$ complexes with N_4 capping ligands to include a mixed valence Fe^{II}−Fe^{III} species. For this series, Fe−O and Fe−Fe distances lengthen as the iron is reduced and/or the μ-O groups are protonated to μ-OH (Figure 2c). Similar trends are likely in MMO and model complexes containing carboxylato groups in the capping ligands. Crystallographic information on such model complexes is limited to [Fe^{III}_2-(μ-OH)$_2$(dipic)$_2$] (**4**)[2] and derivatives,[12] These show longer Fe−Fe distances (3.08 Å) than predicted by the trend line for N_4 capped ligands, suggesting that the nature of the capping ligand influences the geometry of the Fe_2O_2 unit.

Of reported mixed-valence Fe^{II}−Fe^{III} crystal structures,[13] the most closely related (to **1**) core is the Fe_2(μ-OR)$_2$ found in [NEt_4][Fe_2-(salmp)$_2$]·3CH_3CN (**5**).[2,14] In structures of both **1** and **5**, the bond lengths assigned as Fe^{II}−μ-O average 0.17 Å longer than the Fe^{III}−μ-O lengths. The Fe−Fe (3.10 Å) and Fe−μ-O core distances in **5** are all 0.10−0.15 Å longer than in **1**, probably due to the presence of anionic nonbridging ligand groups in **5** (cf. the 3.08 Å Fe−Fe distance in **4** discussed above).

On the basis of the results presented here, complex **1** is a Class II mixed-valence complex by the Robin and Day classification.[15] Observation of an interconversion between **1** and **2** by H-atom transfer would be of interest with respect to elucidating the mechanisms of biological water and dioxygen activation and interconversions.[16]

Acknowledgment. C.J.M. acknowledges support from DANSYNC and the Danish Natural Science Research Council. F.B.L. acknowledges the Siemens Fund, Denmark. XAS were obtained at beam line X18B of the National Synchrotron Light Source, Brookhaven National Laboratory, supported by the U.S. Department of Energy, Division of Materials Sciences and Division of Chemical Sciences. We thank Julio C. de Paula for use of a Jasco V-570 UV/vis/nIR spectrometer purchased with funds from NSF Grant CHE9530707.

Supporting Information Available: CIF file; UV−visible/NIR spectrum, details of fits to XANES and EXAFS (PDF). This material is available free of charge via the Internet at http://pubs.acs.org.

References

(1) (a) Shu, L.; Nesheim, J. C.; Kauffmann, K.; Münck, E.; Lipscomb, J. D.; Que, L., Jr. *Science* **1997**, *275*, 515−518. (b) Que, L., Jr.; Tolman, W. B. *Angew. Chem., Int. Ed.* **2002**, *41*, 1114−1137. (c) MacMurdo, V. L.; Zheng, H.; Que, L., Jr. *Inorg. Chem.* **2000**, *39*, 2254−2255. (d) Zheng, H.; Zang, Y.; Dong, Y.; Young, V. G., Jr.; Que, L., Jr. *J. Am. Chem. Soc.* **1999**, *121*, 2226−2235. (e) Zang, Y.; Pan, G.; Que, L., Jr. *J. Am. Chem. Soc.* **1994**, *116*, 3653−3654. (f) Hsu, H.-F.; Dong, Y.; Shu, L.; Young, V. G., Jr.; Que, L., Jr. *J. Am. Chem. Soc.* **1999**, *121*, 5230−5237.

(2) Ligand abbreviations: 6-Me_3-TPA = tris(6-methyl-2-pyridinemethyl)-amine; BQPA = bis(bis(2-quinolymethyl)−(2-pyridylmethyl)amine; BPEEN = *N*,*N*′-diethyl-*N*,*N*′-bis(2-pyridylmethyl)-ethane-1,2-diamine; 5-Et_3-TPA tris(5-ethylpyrid-2-ylmethyl)amine; dipic = 2,6-pyridinedicarboxylate; salmp = 2-(bis(salicyldeneamino)methyl)phenolate; *N*-MeIm= *N*-methylimidazole.

(3) Wittington, D. A.; Lippard, S. J. *J. Am. Chem. Soc.* **2001**, *123*, 827−838.

(4) Egdal, R. K.; Hazell, A.; McKenzie, C. J., *Acta Crystallogr. C* **2002**, *E58*, m10-m12.

(5) Hazell, R.; Jensen, K. B.; McKenzie, C. J.; Toftlund, H., *J. C. S. Dalton Trans.* **1995**, 707−717.

(6) The compound studied by XANES was determined to be **3** (Poussereau, S.; Blondin, G.; Cesario, M.; Guilhem, J.; Chottard, G.; Gonnet, F.; Girerd, J.-J. *Inorg. Chem.* **1998**, *37*, 3127−3132), rather than the dehydrated form **2** (ref 5) by X-ray crystallography.

(7) Scarrow, R. C.; Brennan, B. A.; Cummings, J. G.; Jin, H.; Duong, D. J.; Kindt, J. T.; Nelson, M. J. *Biochemistry* **1996**, *35*, 10078−10088.

(8) Lee, D.; DuBois, J. L.; Pierce, B.; Hedman, B.; Hodgson, K. O.; Hendrich, M. P.; Lippard, S. J. *Inorg. Chem.* **2002**, *41*, 3172−3182.

(9) Weighted fits to Fourier-filtered $k^3\chi$ follow general procedures outlined in ref 7 and which are detailed in Supporting Information. Uncertainty estimates for EXAFS-derived parameters are by the method of Bunker, G.; Hasnain, S.; Sayers, D. in *X-ray Absorption Fine Structure*; Hasnain, S. S., Ed.; Ellis Horwood: New York, 1991; pp 751−770. The longer Fe−O and Fe−Fe distances have large (ca. 0.1 Å) uncertainties due to correlations with the very similar Fe−N and Fe−C distances, respectively.

(10) Crystallographic data (120K) of **1**: Space group *Aba*2, a = 15.295(1), b = 16.919(1), c = 16.568(1), Z = 4, Siemens SMART CCD diffractometer, $Mo_{K\alpha}$ radiation, graphite monochromator, measured range $2\theta_{max}$ = 59.6° giving, 4607 unique observed reflections. Crystal dimensions 0.44 × 0.36 × 0.20 mm^3, ρ_{calcd} = 1.609 g cm^{-3}, calculation programs: SAINT, SIR97, Krystal. R = 0.041, R_w = 0.044. Residual electron density: −0.37(5) to 0.64(5) e/Å^3.

(11) Allen, F. H.; Kennard, O., *Chem. Design Automation News* **1993**, *8*, 31−37. Found: 19 Fe^{II} complexes and 48 Fe^{III} complexes.

(12) (a) Thich, J. A.; Ou, C. C.; Powers, D.; Vasiliou, B.; Mastropaolo, D.; Potenza, J. A.; Schugar, J. H. *J. Am. Chem. Soc.* **1976**, *98*, 1425−1433. (b) Ou, C. C.; Lalancette, R. A.; Potenza, J. A. *J. Am. Chem. Soc.* **1978**, *100*, 2053−2062.

(13) list of references in supplementary data.

(14) Achim, C.; Bominaar, E. L.; Staples, R. J.; Münck, E.; Holm, R. H. *Inorg. Chem.* **2001**, *40*, 4389−4403.

(15) Robin, M. B.; Day, P. *Adv. Inorg. Radiochem.* **1967**, *10*, 247−422.

(16) Jensen, K. B.; McKenzie, C. J.; Pedersen, J. Z. *Inorg. Chem.* **2001**, *40*, 5066−5067.

JA027219T